Tunable Optical Anisotropy of Seeded CdSe/CdS Nanorods

ARTICLE *in* JOURNAL OF PHYSICAL CHEMISTRY LETTERS · DECEMBER 2013

Impact Factor: 7.46 · DOI: 10.1021/jz402426f

3 AUTHORS, INCLUDING:

Christopher B Murray
University of Pennsylvania
259 PUBLICATIONS **27,590** CITATIONS

THE JOURNAL OF PHYSICAL CHEMISTRY Letters

Letter

pubs.acs.org/JPCL

Tunable Optical Anisotropy of Seeded CdSe/CdS Nanorods

Benjamin T. Diroll,[†] Adriel Koschitzky,[†] and Christopher B. Murray*[,†,‡]

[†]Department of Chemistry, University of Pennsylvania, 231 South 34th Street, Philadelphia, Pennsylvania 19104-6323, United States

[‡]Department of Materials Science and Engineering, University of Pennsylvania, 3231 Walnut Street, Philadelphia, Pennsylvania 19104-6272, United States

Supporting Information

ABSTRACT: We demonstrate structurally tunable optical anisotropy of seeded-growth CdSe/CdS dot-in-rod heterostructures using polarized excitation spectroscopy. The elongated anisotropic CdS shell confers optical anisotropy to the electronic transitions of the CdSe core. Although a rod-shaped shell geometry is a necessary precondition to observing polarized optical properties, the degree of linear polarization is not a strong function of aspect ratio. Rather, tuning the local anisotropy of the emissive core materials by changing the thickness of the anisotropic shell changes the degree of optical anisotropy more dramatically. As the diameter of the core material comprises a greater share (>90%) of the dot-in-rod diameter, the anisotropy of the CdSe core states doubles compared to those for which the core represents <50% of the heterostructure diameter.

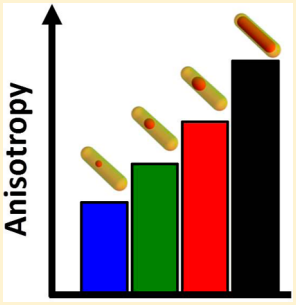

SECTION: Physical Processes in Nanomaterials and Nanostructures

The unique synthetic control and photophysical properties of CdSe/CdS nanoheterostructures make them workhorses of nanoscale science. Starting from quasi-spherical quantum dots (QDs), CdSe/CdS core/shell structures grow in several morphologies, including anisotropic nanorods (NRs).[1] Seeded growth heterostructures have been used to study new synthetic techniques,[1−3] assembly,[3−6] energy-transfer and band structure,[7−9] lasing and gain,[10−12] exciton fine structure,[13] blinking,[14] spin,[15] and polarized optical properties.[16−18] In applied science, CdSe/CdS NRs are potential emitters for luminescent solar concentrators,[19,20] polarized single-molecule bioimaging,[21] and light-emitting diodes.[22] Exploitation of NR heterostructures in light emitting devices across a wide spectral range is contingent on understanding the relationship between microscopic structure and physical properties.

The polarized optical properties of CdSe/CdS dot-in-rods have been reported using several methods. Samples have been studied using stretched polymer films,[2,22] electric fields,[23] photoselection,[16−18] mechanical rubbing,[24] and single-particle polarization measurements have been conducted by several groups, yielding very similar values of emission polarization ($P = (I_{\parallel} - I_{\perp})/(I_{\parallel} + I_{\perp})$) of approximately 0.75.[2,17,25] In this paper we report the tunable polarized optical properties of CdSe/CdS heterostructures using synthetic control of the core and shell materials. For our study, the NRs are made using a "seeded growth" synthesis in which an anisotropic CdS shell is grown from wurtzite QD cores. Controlling seed concentration, crystal structure, reaction temperature, surfactants, and chalcogenide reactivity allows the synthesis of heterostructures with single CdSe "dots" embedded within an anisotropic nanorod shell of tunable aspect ratio.[1−3,26,27] We prepared spherical "small" (2.2 nm), prolate "medium" (3.6 nm × 3.8 nm), and prolate "large" (5.8 nm × 6.8 nm) wurtzite CdSe cores and used these samples as "seeds" to prepare three series of core/shell dot-in-rod samples by seeded growth.[3] CdSe core size, NR aspect ratio, and shell thickness are varied across a series of samples to study the structure−property relationships that dictate optical anisotropy and other photophysical behavior in this heterostructures system.

Figure 1a shows the absorption (solid lines) and photoluminescence (open circles) of the wurtzite CdSe cores with a longest dimension of 2.2 nm (blue), 3.8 nm (green), and 6.8 nm (red). Figure 1b shows absorption and photoluminescence from representative CdSe/CdS NRs made from the three core samples in Figure 1a. Solution-phase X-ray characterization of the same samples follows for the cores in Figure 1c and for the heterostructures in Figure 1d. Small-angle X-ray scattering (SAXS) patterns show ringing characteristic of monodisperse samples.[28] (See Supporting Information Figure S1 for typical transmission electron microscopy images.) The wide-angle patterns show the shift from wurtzite CdSe of the cores to wurtzite CdS of the shell. The preferential *c*-axis growth of the CdS NRs is manifest in the sharp [002] reflection at 27.5° of the dot-in-rod samples. Figure 1d shows the SAXS patterns of the CdSe/CdS NR samples in bold with the corresponding core SAXS pattern shown as a thin line. The patterns in Figure 1d reflect the short axes of the NRs (See Supporting Information Figure S2): ringing features closer to 0° indicate larger rod diameter. Thus the differences between the core and core/shell SAXS patterns reflect the relative thickness of the CdS shell on the core QD. The sample made from the small cores has a thick CdS shell (~1.6 nm), and that made with the

Received: November 10, 2013
Accepted: December 5, 2013
Published: December 9, 2013

   dx.doi.org/10.1021/jz402426f | *J. Phys. Chem. Lett.* 2014, 5, 85−91

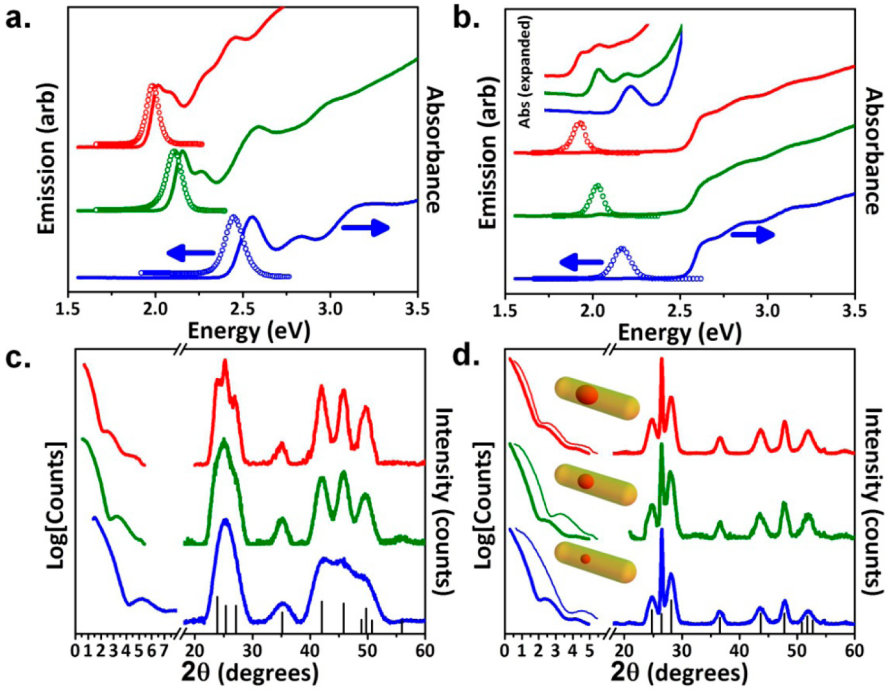

Figure 1. (a) Absorption spectra (solid lines) and emission spectra (open circles) of the small (blue), medium (green), and large (red) quantum dot seeds. (b) Absorption and photoluminescence spectra of seeded-growth core/shell particles made from the seeds in panel a, with the corresponding color. Inset in panel b is the band-edge absorption spectrum of the three samples. (c,d) Small- and wide-angle X-ray scattering data of nanocrystal solutions of the seed particles (c) and core/shell samples (d), in blue (small QDs), green (medium QDs), and red (large QDs). Thin lines in panel d are reproductions of the small-angle scattering from the core samples, and thick lines represent scattering from the core/shell heterostructures. Stick patterns represent wurtzite CdSe (c) and wurtzite CdS (d). Curves are offset for clarity.

largest core has a thin shell (<0.5 nm). Elemental analysis[1] and high-resolution TEM[3] have suggested that the core material sits asymmetrically within the nanorod shell (as shown in the cartoons of Figure 1), although there is little known about the statistical distribution of cores within large populations.

The thickness of the CdS shell is known to influence the photophysical properties of CdSe/CdS nanostructures, including quantum yield,[20] lifetime,[20] and blinking.[14] Using polarized excitation spectroscopy, we have also found that the thickness of the CdS shell plays a major role in the polarized optical properties of CdSe/CdS dot-in-rods. Although wurtzite QDs are slightly prolate, they still do not show steady state optical anisotropy,[16,18] although at short times they show fluorescence with dynamic albeit relatively weak polarization properties.[29] Encapsulation within an anisotropic shell yields large, positive optical anisotropy in steady state measurements. Using photoselection with a horizontal (H) or vertical (V) polarizer to selectively excite those fluorophores aligned with the excitation source, we then monitor the emission of the selected subpopulation through a vertical polarizer. Unlike molecular spectroscopy, rotational depolarization of NRs is very slow (>1 μs) compared to the fluorescence lifetime (10−50 ns), and measurements can be performed at room temperature in hexanes. Adjusting for the monochromator intensity (I) throughput of vertical or horizontal light using a factor $G = I_{HV}/I_{HH}$, we obtain the anisotropy (R) of a sample[30]

$$R = \frac{I_{\parallel} - I_{\perp}}{I_{\parallel} + 2I_{\perp}} = \frac{I_{VV} - GI_{VH}}{I_{VV} - 2GI_{VH}} \tag{1}$$

As we showed in an earlier publication, measuring anisotropy as a function of excitation energy allows a deconvolution of the anisotropy R_i associated with transition i of the excitation spectrum.[18] The application of this fitting procedure for three CdSe/CdS dot-in-rod samples with different core sizes is shown in Figure 2. First, the photoluminescence excitation spectrum from the band edge to ~2.6 eV is fitted with Gaussian curves to model transitions (A_i) expected from Norris and Bawendi (see SI).[31] An additional Gaussian peak (show in magenta) is added, centered at 2.6 eV to model absorption into the first CdS shell state apparent in the absorption spectra in Figure 1b. The total excitation intensity is modeled as

$$I_{PLE}(E) = I_{\parallel} + 2GI_{\perp} = \sum_i A_i(E) \tag{2}$$

The first row of Figure 2 shows the fitted excitation data, with the same electronic transitions represented by the same curve color. The experimental data are plotted in blue (small cores), green (medium), and red circles (large) and the yellow curve represents the cumulative fit of Gaussians.

Second, each of these excitation transitions i is assigned an energy-dependent probability, defined as $F_i(E) = A_i(E)/I_{PLE}(E)$. The values for $F_i(E)$, shown in the second row of Figure 2, represent the probability of exciting a particular transition i as a function of energy. Finally, these energy-dependent probabilities can be used as the basis set to fit the anisitropy (R) measured by photoselection. Anisotropy is the sum of the anisotropy of each contributing fluorophore, so we use the energy-dependent probabilities $F_i(E)$ as the basis functions to deconvolute the anisotropy of each transition, R_i, according to eq 3:

$$R(E) = \sum_i R_i F_i(E) \tag{3}$$

dx.doi.org/10.1021/jz402426f | J. Phys. Chem. Lett. 2014, 5, 85−91

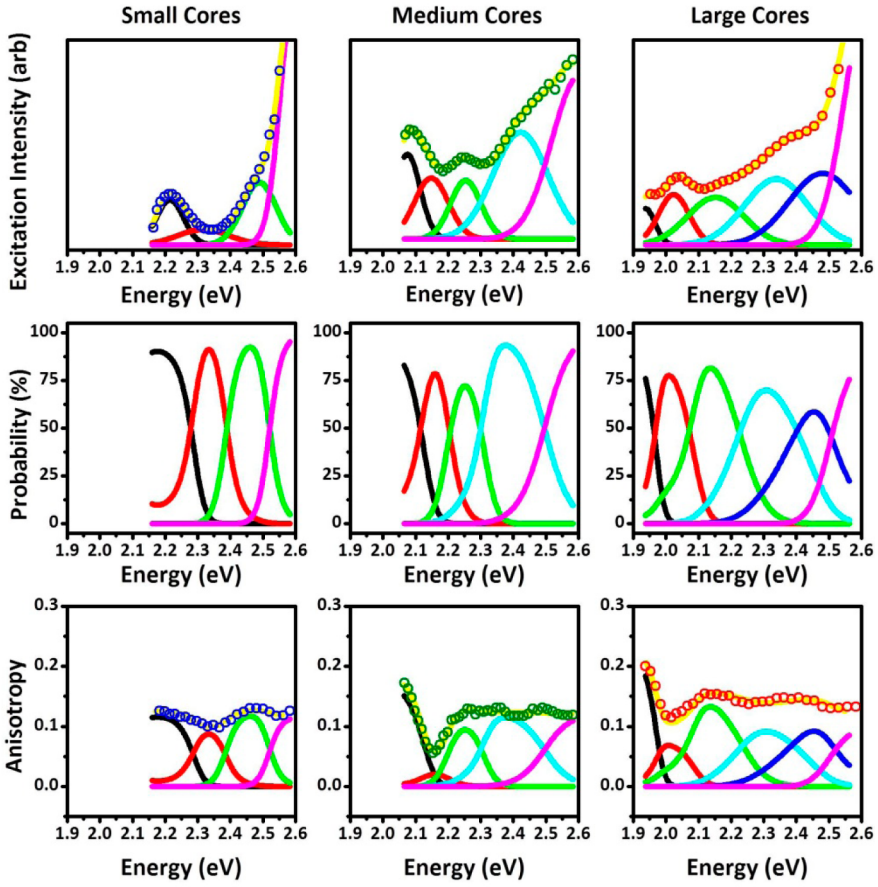

Figure 2. The columns demonstrate the three-step fitting procedure for interpreting polarized excitation measurements for the small-, medium-, and large-core seeded CdSe/CdS NRs. The first row shows the polarization-weighted excitation data of the samples in open circles fitted with the yellow cumulative fit line. The color of the lines fitting the excitation features (black, red, green, cyan, blue, and magenta) is maintained between columns and rows, representing the transitions i of the CdSe/CdS electronic structure. The second row shows the probability of absorption into each of the fitted states as a function of energy. The third row shows the anisotropy spectrum in open circles fitted by using the probability functions of the second row weighted by the anisotropy of each state, with the cumulative fit in yellow.

The last row of Figure 2 shows the experimentally measured anisotropy in open circles, fitted according to eq 3. The yellow curve represents the cumulative fit and each of the colored curves represents $R_iF_i(E)$.

Figure 3a shows the numerical result of the fitting procedure for the three samples analyzed in Figures 1 and 2. The fitted values of R_i are plotted for the four common excitation features shared by the small, medium, and large core samples. Figure 3b shows the classical excitonic absorptions of CdSe QDs: the common excitations correspond with the black ($1S_{3/2}-1S_e$), red ($2S_{3/2}-1S_e$), green ($1P_{3/2}-1P_e$), and magenta ($CdS_{VB}-CdS_{CB}$) curves in Figure 2. A few results are noteworthy: the anisotropy measured at the first excitation feature increases with the size of the CdSe seed and correlates inversely with the relative shell thickness. The $1S_{3/2}-1S_e$ excitation anisotropy is ~0.13 for the small core sample but reaches ~0.24 for the largest core sample in Figure 3a. Samples with CdSe NR cores show the same pattern with even higher band-edge anisotropy (see Supporting Information). Second, the samples all show the highest polarization at the band edge, which decreases in the second transition, and increases for the third, reflecting their similar electronic structure. Last, the anisotropy of the CdS band-edge absorption feature is similar in all samples.

The synthesis of many samples with different core sizes allows for tests of measurable photophysical behavior and structure–property correlations. Using 15 new samples—five with each size of core—we track the structure-dependent optical properties of the dot-in-rod heterostructures. Using TEM, we determined the thickness and aspect ratio of each dot-in-rod sample (see Supporting Information). Absorption redshifts are known to depend strongly on the rod shell diameter for a fixed core size.[13] Figure 3c shows a very similar result by showing the photoluminescence redshift from the core to core/shell samples: samples in which the core material makes up the largest fraction of the total diameter have <50 meV redshifts of the emission, whereas those in which the shell is a large fraction of the diameter (>50%) have redshifts as large as 300 meV. The results are similar to the reported redshifts in CdSe/CdS QDs.[33] The sharp photoluminescence (as small as 75 meV fwhm) and the high correlation of the shell thickness with the optical redshift is an indication that the optical energies are only weakly affected by the nanorod dimensions, consistent with confinement of the electron only in the short dimensions of the quasi-1D shell. These properties also suggest that the results are not strongly dependent on the position of the emissive CdSe seed in the CdS shell.

We have also analyzed the relation of the physical dimensions of the NRs to their optical anisotropy observed using photoselection. The values of the anisotropy plotted in Figures 3d and 3e are from the curves in Supporting

dx.doi.org/10.1021/jz402426f | J. Phys. Chem. Lett. 2014, 5, 85–91

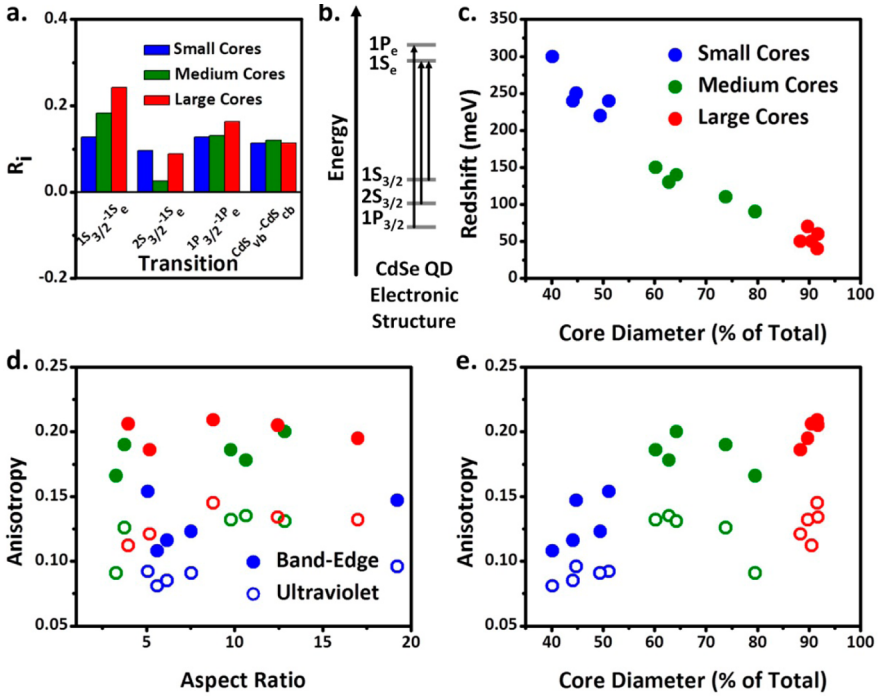

Figure 3. (a) Anisotropies R_i plotted for the three lowest-energy CdSe QD excitations, shown in (b),[32] and the CdS excitation of the CdSe/CdS dot-in-rod structures. These are the results of the fitting procedure in Figure 2. (c) Photoluminescence redshift is plotted against the fraction of the heterostructure diameter made up by the core material. Anisotropy at the band edge (filled circles) and the ultraviolet (open circles) is plotted against aspect ratio (d) and the relative core diameter (e).

Information Figure S3. The energy-dependent anisotropy of each series of core/shell NRs is similar, showing the common structure for each core particle. Filled circles show the values of anisotropy measured at the band-edge and open circles show the values measured for excitation at 3.5 eV. Figure 3d shows the anisotropy plotted against the aspect-ratio of the NRs. Although the elongation of the shell material is essential for observing optical anisotropy, at aspect ratios greater than 2, there is little effect on the polarization properties of the dot-in-rod samples. Insensitivity of the optical polarization to the aspect ratio above a threshold value is observed in CdSe NRs as well.[34] Figure 3e highlights a far more important determinant of polarized optical properties for the dot-in-rod samples: the shell thickness of the core/shell dot-in-rod samples is negatively correlated with increased anisotropy, both for the anisotropy in the ultraviolet and at low energies. This is observable, but less clear within the series of core samples, likely because the correlation is perturbed by the noise and of the measurement and even small errors in size estimation. Observing the samples taken together, the relative structural anisotropy of the local environment of the CdSe core more clearly dictates the optical anisotropy of the dot-in-rod heterostructure.

Anisotropy of isotropically dispersed, cylindrically symmetrical fluorophores measured using photoselection, as described in this paper, is a function of both anisotropy of absorption (defined as $r = (r_{\|} - r_{\perp})/(r_{\|} + r_{\perp})$) and anisotropy of emission ($q = (q_{\|} - q_{\perp})/(q_{\|} + 2q_{\perp})$), according to[18,35]

$$R = \frac{2}{5}rq \tag{4}$$

In contrast to earlier measurements,[23,36] direct measurements of the excitation and emission polarization properties are not obtained. Thus the trends in the anisotropy observed in Figure 3 cannot be unambiguously assigned to changes in the polarization of the emission, absorption, or both. To overcome this problem, we use the dielectric ellipsoid model to estimate absorption anisotropy r.

Because NR emission derives from the same transitions regardless of the excitation energy (for single excitons), the anisotropy of the emission is fixed. The anisotropy of absorption depends, however, on the energy of excitation and the particular transitions which are excited. Under the dielectric ellipsoid model, the cross-section of an electronic absorption, generally $\sigma \propto \langle i|\mathbf{p}|f\rangle|^2\ (\varepsilon_{\text{medium}}/(1-\alpha)\varepsilon_{\text{medium}} - \varepsilon_{\text{rod}})^2$,[23,37] can be reduced to the dielectric term at high energies. The electronic transition dipoles ($i|\mathbf{p}|f$) show no preferential directionality because they derive from many closely spaced, overlapping states with different symmetries. The factor α depends on the dielectric and aspect ratio of the rod and the dielectric medium (see SI), with $\alpha_{\|} \neq \alpha_{\perp}$. Colloidal NRs act as miniature bar polarizers, preferentially attenuating incident electric fields polarized perpendicular to the long axis. Absorption polarization from the NR dielectric is the reason for the flat, positive values of anisotropy in the UV observed in Figure S3. Applying dielectric models allows a reasonable estimate of the absorption polarization in the ultraviolet.[16,23,38] Using the dielectric estimate of r and the measured value of anisotropy (R), we obtain an estimate of the emission polarization of the dot-in-rod samples using eq 4. (Full details are in the Supporting Information.)

Open circles in Figure 4a show the estimated emission polarization for the samples of small (blue), medium (green), and large (red) core CdSe/CdS heterostructures. Filled circles show the value of absorption anisotropy at the band-edge using the measured value of R and the estimated value of q according to eq 4. Although the dielectric ellipsoid model yields, in 2 of 15 cases, the nonphysical result that band-edge absorption polarization is lower than emission polarization, the general

dx.doi.org/10.1021/jz402426f | J. Phys. Chem. Lett. 2014, 5, 85−91

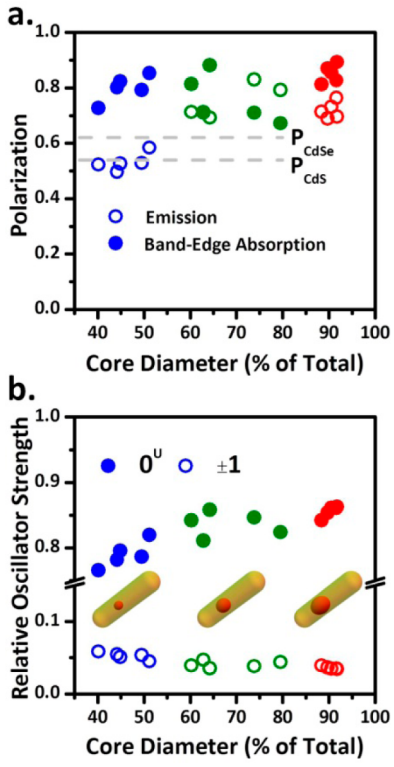

Figure 4. (a) Emission polarization and band-edge polarization predicted according to the dielectric ellipsoid model for CdSe/CdS dot-in-rod samples made with small (blue), medium (green), and large (red) CdSe cores. Dashed lines indicate the polarization expected for an infinite wire of CdSe or CdS in an $\varepsilon = 2$ environment. (b) Relative oscillator strength of the 0^U and ±1 excitonic states in the lowest electronic state of the same CdSe/CdS NR samples.

pattern is reasonable and corresponds well with the data in Figure 3 and literature measurements of emission polarization of CdSe/CdS dot-in-rod structures.[25] The degree of polarization increases as the relative shell thickness of the dot-in-rod sample decreases, but the data collected in Figure 3 and modeled in here suggests that the band-edge polarization of the dot-in-rod samples is limited to a maximum of ~0.8. We were unable to obtain band-edge polarizations >0.9 except by using a CdSe nanorod core in a CdSe/CdS rod-in-rod structure (Figure S6).

The dashed lines in Figure 4a indicate the polarization expected for a wire of CdSe or CdS in a low dielectric ($\varepsilon = 2$) environment; estimations of the polarization greater than these values are suggestive of the role of the quantum confined electronic structure in the band-edge polarization. The photoluminescence and band-edge absorption feature of CdSe nanostructures contains eight finely spaced energy levels for the lowest-energy exciton.[13,39] In wurtzite CdSe QDs, two of these exciton fine structure states are optically passive; four states ($\pm1^L$ for lower and $\pm1^U$ for upper transitions) have angular momentum and represent circularly polarized transitions in the *ab*-plane of the wurtzite crystal; and one state, 0^U, is linearly polarized along the wurzite *c*-axis, which is also the long-axis of CdSe/CdS NRs (Figure 1d).

Although CdSe/CdS dot-in-plate structures have shown large splitting of the exciton fine structure states which explains band-edge polarization properties,[40] Raino et al. demonstrated that splitting of exciton fine structure states is much smaller in dot-in-rod structures compared to QDs (Figure S7).[13] The band-edge polarization properties of CdSe/CdS dot-in-rod samples are a function of the tunable oscillator strength of the linearly polarized excitation and emission compared to the ±1 transitions.[41] Previous reports have suggested that the anisotropic pressure on the CdSe core from the lattice mismatch with the CdS shell can be responsible for linear (for dot-in-rod samples) and planar (for dot-in-plate samples) emission polarization.[2,40] To this we add that the degree of polarization depends on the degree to which the pressure is anisotropically distributed on the core particle. Figure 4b shows the empirically estimated oscillator strength of the 0 and ±1 exciton fine structure states, consistent with the average of band-edge absorption and emission polarization in Figure 4a. The oscillator strength differences plotted in Figure 4b subsume both the polarization conferred by the anisotropic dielectric nanorod, which is similar between all samples, and the polarization conferred by the specific directionality of the electronic transitions due to the anisotropic pressure exerted by the lattice shell.[2,40] Even for rods of similar aspect ratio, the changes in the relative oscillator strength of band-edge transitions tune the optical anisotropy of the samples.

In summary, we have demonstrated that by tuning the degree of anisotropy of the environment surrounding the emissive CdSe of CdSe/CdS dot-in-rod nanostructures, we tune the degree of optical anisotropy observed for the samples. Dot-in-rod nanostructures can be made with shells of variable thickness to tune the degree of linear polarization of the electronic transitions. Our finding that the degree of polarization in CdSe/CdS dot-in-rod heterostructures is strongly correlated with the thickness of the CdS shell along the short axis suggests that higher degrees of optical anisotropy may face a trade-off with blinking, brightness, stability, and emission color. Thicker shells frequently used to passivate QDs for less blinking and higher quantum yield are also likely to yield a more isotropic electronic landscape for the emissive core material, and thus lower optical anisotropy.

■ ASSOCIATED CONTENT

Supporting Information

Supporting Information includes more on experimental methods, transmission electron microscopy, anisotropy data, time-resolved photoluminescence, sample sizing information, and supporting mathematics. This material is available free of charge via the Internet at http://pubs.acs.org.

■ AUTHOR INFORMATION

Corresponding Author

*E-mail: cbmurray@sas.upenn.edu.

Notes

The authors declare no competing financial interest.

■ ACKNOWLEDGMENTS

The authors would like to thank Yale E. Goldman for access to equipment used in this research. B.T.D., A.K., and C.B.M. acknowledge support from DOE Office of Basic Sciences under award No. DE-SC0002158. A.K. acknowledges support from the Provost's office at the University of Pennsylvania through the Penn Undergraduate Mentor Research program and B.T.D. acknowledges support from the I.B.M. Ph. D. Fellowship. C.B.M. is grateful for the Richard Perry University Professorship at the University of Pennsylvania.

REFERENCES

(1) Talapin, D. V; Nelson, J. H.; Shevchenko, E. V; Aloni, S.; Sadtler, B.; Alivisatos, A. P. Seeded Growth of Highly Luminescent CdSe/CdS Nanoheterostructures with Rod and Tetrapod Morphologies. *Nano Lett.* **2007**, *7*, 2951−2959.

(2) Talapin, D. V.; Koeppe, R.; Götzinger, S.; Kornowski, A.; Lupton, J. M.; Rogach, A. L.; Benson, O.; Feldmann, J.; Weller, H. Highly Emissive Colloidal CdSe/CdS Heterostructures of Mixed Dimensionality. *Nano Lett.* **2003**, *3*, 1677−1681.

(3) Carbone, L.; Nobile, C.; De Giorgi, M.; Della Sala, F.; Morello, G.; Pompa, P.; Hytch, M.; Snoeck, E.; Fiore, A.; et al. Synthesis and Micrometer-Scale Assembly of Colloidal CdSe/CdS Nanorods Prepared by a Seeded Growth Approach. *Nano Lett.* **2007**, *7*, 2942−2950.

(4) Talapin, D. V; Shevchenko, E. V; Murray, C. B.; Kornowski, A.; Förster, S.; Weller, H. CdSe and CdSe/CdS Nanorod Solids. *J. Am. Chem. Soc.* **2004**, *126*, 12984−12988.

(5) Wang, T.; Zhuang, J.; Lynch, J.; Chen, O.; Wang, Z.; Wang, X.; LaMontagne, D.; Wu, H.; Cao, Y. C. Self-Assembled Colloidal Superparticles from Nanorods. *Science* **2012**, *338*, 358−363.

(6) Pietra, F.; Rabouw, F. T.; Evers, W. H.; Byelov, D. V; Petukhov, A. V; de Mello Donegá, C.; Vanmaekelbergh, D. Semiconductor Nanorod Self-Assembly at the Liquid/Air Interface Studied by in situ GISAXS and ex situ TEM. *Nano Lett.* **2012**, *12*, 5515−5523.

(7) Steiner, D.; Dorfs, D.; Banin, U.; Della Sala, F.; Manna, L.; Millo, O. Determination of Band Offsets in Heterostructured Colloidal Nanorods Using Scanning Tunneling Spectroscopy. *Nano Lett.* **2008**, *8*, 2954−2958.

(8) Sitt, A.; Della Sala, F.; Menagen, G.; Banin, U. Multiexciton Engineering in Seeded Core/Shell Nanorods: Transfer from Type-I to Quasi-Type-II Regimes. *Nano Lett* **2009**, *9*, 3470−3476.

(9) Rainò, G.; Stöferle, T.; Moreels, I.; Gomes, R.; Kamal, J. S.; Hens, Z.; Mahrt, R. F. Probing the Wave Function Delocalization in CdSe/CdS Dot-in-Rod Nanocrystals by Time- and Temperature-Resolved Spectroscopy. *ACS Nano* **2011**, *5*, 4031−4036.

(10) Krahne, R.; Zavelani-Rossi, M.; Lupo, M. G.; Manna, L.; Lanzani, G. Amplified Spontaneous Emission from Core and Shell Transitions in CdSe/CdS Nanorods Fabricated by Seeded Growth. *Appl. Phys. Lett.* **2011**, *98*, 063105−1−063105−3.

(11) Liao, Y.; Xing, G.; Mishra, N.; Sum, T. C.; Chan, Y. Low Threshold, Amplified Spontaneous Emission from Core-Seeded Semiconductor Nanotetrapods Incorporated into a Sol−Gel Matrix. *Adv. Mater.* **2012**, *24*, OP159−OP164.

(12) Xing, G.; Liao, Y.; Wu, X.; Chakrabortty, S.; Liu, X.; Yeow, E. K. L.; Chan, Y.; Sum, T. C. Ultralow Threshold Two-Photon Pumped Amplified Spontaneous Emission and Lasing from Seeded CdSe/CdS Nanorod Heterostructures. *ACS Nano* **2012**, *6*, 10835−10844.

(13) Rainò, G.; Stöferle, T.; Moreels, I.; Gomes, R.; Hens, Z.; Mahrt, R. F. Controlling the Exciton Fine Structure Splitting in CdSe/CdS Dot-in-Rod Nanojunctions. *ACS Nano* **2012**, *6*, 1979−1987.

(14) Pisanello, F.; Leménager, G.; Martiradonna, L.; Carbone, L.; Vezzoli, S.; Desfonds, P.; Cozzoli, P. D.; Hermier, J.-P.; Giacobino, E.; Cingolani, R.; et al. Non-Blinking Single-Photon Generation with Anisotropic Colloidal Nanocrystals: Towards Room-Temperature, Efficient, Colloidal Quantum Sources. *Adv. Mater.* **2013**, *25*, 1973−1973.

(15) Lupton, J. M.; Talapin, D. V; Huang, J.; Boehme, C.; van Schooten, K. J.; Baker, W. Spin-Dependent Exciton Quenching and Spin Coherence in CdSe/CdS Nanocrystals. *Nano Lett.* **2012**, *13*, 65−71.

(16) Sitt, A.; Salant, A.; Menagen, G.; Banin, U. Highly Emissive Nano Rod-in-Rod Heterostructures with Strong Linear Polarization. *Nano Lett.* **2011**, *11*, 2054−2060.

(17) Hadar, I.; Hitin, G. B.; Sitt, A.; Faust, A.; Banin, U. Polarization Properties of Semiconductor Nanorod Heterostructures: From Single Particles to the Ensemble. *J. Phys. Chem. Lett.* **2013**, *4*, 502−507.

(18) Diroll, B. T.; Dadosh, T.; Koschitzky, A.; Goldman, Y. E.; Murray, C. B. Interpreting the Energy-Dependent Anisotropy of Colloidal Nanorods Using Ensemble and Single-Particle Spectroscopy. *J. Phys. Chem. C* **2013**, *117*, 23928−23937.

(19) Barnham, K.; Marques, J. L.; Hassard, J.; O'Brien, P. Quantum-Dot Concentrator and Thermodynamic Model for the Global Redshift. *Appl. Phys. Lett.* **2000**, *76*, 1197−1199.

(20) She, C.; Demortière, A.; Shevchenko, E. V.; Pelton, M. Using Shape to Control Photoluminescence from CdSe/CdS Core/Shell Nanorods. *J. Phys. Chem. Lett.* **2011**, *2*, 1469−1475.

(21) Deka, S.; Quarta, A.; Lupo, M. G.; Falqui, A.; Boninelli, S.; Giannini, C.; Morello, G.; De Giorgi, M.; Lanzani, G.; Spinella, C.; Cingolani, R.; Pellegrino, T.; Manna, L. CdSe/CdS/ZnS Double Shell Nanorods with High Photoluminescence Efficiency and Their Exploitation as Biolabeling Probes. *J. Am. Chem. Soc.* **2009**, *131*, 2948−2958.

(22) Hikmet, R. A. M.; Chin, P. T. K.; Talapin, D. V.; Weller, H. Polarized-Light-Emitting Quantum-Rod Diodes. *Adv. Mater.* **2005**, *17*, 1436−1439.

(23) Kamal, J.; Gomes, R.; Hens, Z.; Karvar, M.; Neyts, K.; Compernolle, S.; Vanhaecke, F. Direct Determination of Absorption Anisotropy in Colloidal Quantum Rods. *Phys. Rev. B* **2012**, *85*, 035126-1−035126-7.

(24) Amit, Y.; Faust, A.; Lieberman, I.; Yedidya, L.; Banin, U. Semiconductor Nanorod Layers Aligned through Mechanical Rubbing. *Phys. Status Solidi A* **2012**, *209*, 235−242.

(25) Pisanello, F.; Martiradonna, L.; Spinicelli, P.; Fiore, A.; Hermier, J. P.; Manna, L.; Cingolani, R.; Giacobino, E.; De Vittorio, M.; Bramati, A. Dots in Rods as Polarized Single Photon Sources. *Superlattices Microstruct.* **2010**, *47*, 165−169.

(26) Huang, J.; Kovalenko, M. V; Talapin, D. V. Alkyl Chains of Surface Ligands Affect Polytypism of CdSe Nanocrystals and Play an Important Role in the Synthesis of Anisotropic Nanoheterostructures. *J. Am. Chem. Soc.* **2010**, *132*, 15866−15868.

(27) Ruberu, T. P. A.; Albright, H. R.; Callis, B.; Ward, B.; Cisneros, J.; Fan, H.-J.; Vela, J. Molecular Control of the Nanoscale: Effect of Phosphine−Chalcogenide Reactivity on CdS−CdSe Nanocrystal Composition and Morphology. *ACS Nano* **2012**, *6*, 5348−5359.

(28) Murray, C. B.; Kagan, C. R.; Bawendi, M. G. Synthesis and Characterization of Monodisperse Nanocrystals and Close-Packed Nanocrystal Assemblies. *Annu. Rev. Mater. Sci.* **2000**, *30*, 545−610.

(29) Bawendi, M. G.; Carroll, P. J.; Wilson, W. L.; Brus, L. E. Luminescence Properties of CdSe Quantum Crystallites: Resonance Between Interior and Surface Localized States. *J. Chem. Phys.* **1992**, *96*, 946−954.

(30) Lakowicz, J. *Principles of Fluorescence Spectroscopy*, 2nd ed.; Springer: New York, 2004; pp 291−319.

(31) Norris, D.; Bawendi, M. Measurement and Assignment of the Size-Dependent Optical Spectrum in CdSe Quantum Dots. *Phys. Rev. B* **1996**, *53*, 16338−16346.

(32) Kim, J.; Wong, C. Y.; Scholes, G. D. Exciton Fine Structure and Spin Relaxation in Semiconductor Colloidal Quantum Dots. *Acc. Chem. Res.* **2009**, *42*, 1037−1046.

(33) Van Embden, J.; Jasieniak, J.; Mulvaney, P. Mapping the Optical Properties of CdSe/CdS Heterostructure Nanocrystals: The Effects of Core Size and Shell Thickness. *J. Am. Chem. Soc.* **2009**, *131*, 14299−14309.

(34) Hu, J.; Li, L.-S.; Yang, W.; Manna, L.; Wang, L.-W.; Alivisatos, A. P. Linearly Polarized Emission from Colloidal Semiconductor Quantum Rods. *Science* **2001**, *292*, 2060−2063.

(35) Klinger, D. S.; Lewis, J. W.; Einterz, R. C. *Polarized Light in Optics and Spectroscopy*, 1st ed.; Academic Press: San Diego, CA, 1990; pp 153−236.

(36) McDonald, M. P.; Vietmeyer, F.; Kuno, M. Direct Measurement of Single CdSe Nanowire Extinction Polarization Anisotropies. *J. Phys. Chem. Lett.* **2012**, *3*, 2215−2220.

(37) Merzbacher, E. *Quantum Mechanics*; Wiley: New York, 1970; pp 463−470.

(38) Lan, A.; Giblin, J.; Protasenko, V.; Kuno, M. Excitation and Photoluminescence Polarization Anisotropy of Single CdSe Nanowires. *Appl. Phys. Lett.* **2008**, *92*, 183110.

(39) Norris, D.; Efros, A.; Rosen, M.; Bawendi, M. Size Dependence of Exciton Fine Structure in CdSe Quantum Dots. *Phys. Rev. B* **1996**, *53*, 16347−16354.
(40) Cassette, E.; Mahler, B.; Guigner, J.-M.; Patriarche, G.; Dubertret, B.; Pons, T. Colloidal CdSe/CdS Dot-in-Plate Nanocrystals with 2D-Polarized Emission. *ACS Nano* **2012**, *6*, 6741−6750.
(41) Shabaev, A.; Efros, A. L. 1D Exciton Spectroscopy of Semiconductor Nanorods. *Nano Lett.* **2004**, *4*, 1821−1825.

dx.doi.org/10.1021/jz402426f | *J. Phys. Chem. Lett.* 2014, 5, 85−91